Chemical Engineering Communications

ISSN: 0098-6445 (Print) 1563-5201 (Online) Journal homepage: https://www.tandfonline.com/loi/gcec20

PHOTOINDUCED WETTABILITY OF TITANIUM OXIDE THIN FILMS

Diana Mardare , Alina Manole , A. Yıldız & D. Luca

To cite this article: Diana Mardare , Alina Manole , A. Yıldız & D. Luca (2010) PHOTOINDUCED WETTABILITY OF TITANIUM OXIDE THIN FILMS, Chemical Engineering Communications, 198:4, 530-540, DOI: 10.1080/00986445.2010.512531

To link to this article: https://doi.org/10.1080/00986445.2010.512531

Chem. Eng. Comm., 198:530–540, 2011

ISSN: 0098-6445 print/1563-5201 online
DOI: 10.1080/00986445.2010.512531

Taylor & Francis
Taylor & Francis Group

Photoinduced Wettability of Titanium Oxide Thin Films

DIANA MARDARE,[1] ALINA MANOLE,[1] A. YILDIZ,[2] AND D. LUCA[1]

[1]Faculty of Physics, Alexandru Ioan Cuza University, Iaşi, Romania
[2]Faculty of Science and Arts, Department of Physics, Ahi Evran University, Kirsehir, Turkey

We present here the results of a systematic investigation of the influence of the main deposition parameters (substrate temperature, deposition time, reactive gas composition, etc.) on the hydrophilic properties of DC sputtered titania films, grown on heated glass substrates (463−573 K), using water vapors as the reactive gas. Reference samples prepared in standard oxygen-based deposition conditions were used to compare the results. All the investigated samples were polycrystalline, with either pure anatase or mixed anatase-rutile nano-phase mixtures, depending on substrate temperature and film thickness. The surface wettability, evaluated from contact angle data during UV irradiation and in the back-reaction conditions, is discussed in terms of the synergic effects of materials structure, surface morphology, elemental composition, and electronic properties.

Keywords Contact angle; Hydrophilicity; Reactive DC sputtering; Thin films; TiO_2; Water vapor

Introduction

It is well known that wide-gap titanium dioxide can degrade organic pollutants in water, air, or on solid surfaces. Particle and film titania-based photocatalysts are currently used to remedy the waste-contaminated water and to manufacture self-cleaning dyes in outdoor applications (Ollis et al., 1993). Powder photo-catalytic materials have many drawbacks compared with thin films, the most important one being the need to recover it from solution at the end of the process. Therefore, in this paper we deal with titania thin films.

Among the TiO_2 polymorphs in thin films, anatase is the most active, due to its largest optical gap (3.2 eV) compared to rutile (3.0 eV) (Hashimoto et al., 2005). Detailed investigations to elucidate the basic surface chemistry of titania have been reported, mainly on rutile (Hashimoto et al., 2005), but also on anatase single-crystalline surfaces (Ruzycki et al., 2003). The beneficial photocatalytic and hydrophilic features of the pristine titania materials are based on the role played by the long lifetime values of the electron-hole pairs occurring under UV irradiation in

Address correspondence to Diana Mardare, Faculty of Physics, Alexandru Ioan Cuza University, 11, Carol I Blvd., 700506 Iaşi, Romania. E-mail: dianam@uaic.ro

the surface region. It has been demonstrated that the lifetime values are directly proportional to the bandgap values (Hao et al., 2002).

One of the main factors affecting the photocatalytic efficiency of the technologically important titania materials is the percentage of the anatase phase and the large specific area of the active catalyst fraction. For application purposes, tailoring materials properties frequently require a rapid assessment of the photocatalytic activity. Evaluating the reaction rate constants of the oxidation processes at the photo-catalytic surface involves long-duration measurements. Therefore, assessing the surface wettability may represent a more rapid converse procedure, as long as the surface hydrophilicity/hydrophobicity are intimately associated with the oxidizing efficiency (despite the fact that wettability and oxidation activity in titania materials rely on different mechanisms (Fujishima et al., 1999; Shirolkar et al., 2008; Mardare et al., 2007a; Luca et al., 2007; Mardare et al., 2007b).

We report in this paper on the hydrophilicity properties of DC sputter-deposited TiO_2 thin films prepared with water vapors as reactive gas in the discharge, and compare the results with those of classically grown films using oxygen as reactive gas. The relation between film wettability and thickness, structure, surface morphology, and elemental composition is discussed below in relation with the deposition parameters. The results demonstrate the potential benefit of using the investigated films as supported photocatalysts for applications in surface self-cleaning.

Experimental

The DC discharge using a metallic Ti cathode-target (99.5% purity, 60 mm diameter) was used to grow titanium oxide films on rotating glass substrates. As demonstrated in Mardare et al. (2000) and Musil et al. (2006), substrate temperature and film thickness are key factors to grow nano-crystalline films. Therefore, films of various thicknesses were deposited on heated substrates. The target-to-film substrates distance was 150 mm in all deposition runs, to ensure appropriate film uniformity. The partial pressure of water vapors or oxygen in the discharge was maintained at 0.6×10^{-3} mbar, while the Ar partial pressure was 1.4×10^{-3} mbar. The plasma conditions were monitored in terms of gas composition with a quadrupole mass spectrometer operated in residual gas analyzer regime (Balzers QMG 125).

The discharge current was operated in constant current mode (0.4 A) therefore the DC power has changed between 200 and 230 W upon the changes in target surface conditions. Additional deposition parameters are presented in detail in Table I.

Film thickness was measured using a stylus profilometer (Tencor Alpha-Step 500). The XRD patterns obtained at 5° grazing incidence diffraction (Rigaku Geigerflex diffractometer, using the CuK_α radiation, $\lambda = 1.540591$ Å) were used to derive average crystallite size values of the phases occurring in the films. The diffraction peaks were indexed using the JCPDS cards no. 78–2486 for antase and no. 87-0920 for rutile.

The weight percentage of the anatase phase (W_A) in the films was calculated according to the procedure introduced in Mardare et al. (2000) by using the Spurr equation (Spurr and Myers, 1957):

$$W_A = 1/(1 + 1.265 I_R/I_A), \quad (1)$$

Table I. Substrate temperature (T_S), deposition time (t), thickness of the films (d), weight percentage of anatase phase (W_A), average crystallite sizes for the anatase (D_A), rutile (D_R) phases, root mean square roughness (R_{rms}), optical band gap (E_g)

Sample	Reactive gas	T_S (K)	t (min)	d (nm)	W_A (%)	D_A (nm)	D_R (nm)	R_{rms} (nm)	E_g (eV)
S.AR1	H_2O	573	255	260	46	20	15	8.8	3.22
S.AR2	H_2O	573	420	429	46	22	17	11.5	3.22
S.AR3	H_2O	463	472	300	46	13	11	3.1	3.19
S.A	H_2O	523	372	260	97	12	6	4.7	3.24
S.RA	O_2	573	300	200	28	29	17	3.1	3.05

where I_R and I_A are the intensities of the most intense peaks: rutile R(110) and anatase A(101). The average crystallite size was calculated using the same diffraction peaks, using the Scherrer equation (Klug and Alexander, 1974):

$$D = 0.9\lambda/(B_{1/2}cos\theta), \tag{2}$$

where $B_{1/2}$ is the diffraction peak width (in radians), θ – the Bragg angle, and λ – the X-ray wavelength.

The surface morphology of the films was investigated by atomic force microscopy (AFM, Topometrics Explorer) in non-contact mode. The hydrophilic properties of the films were investigated by contact angle measurements (CAM) of de-ionized water with film surface in a sessile drop arrangement using a Data Physics OCA 15C goniometer. All the CAMs were done under the conditions of 25°C room temperature and 60% relative humidity. Drop volume values of 500 nanoliters were chosen to diminish the effects of water evaporation during CAM and to avoid drop shape alteration due to gravitational forces.

Sample UV irradiation was done using a non-filtered 150 W high-pressure Hg lamp ensuring a flux of 10 mW/cm^2 at the investigated surface. During CAM, the contact angle was monitored against the incident UV dose (at five different locations on the film's surface), until the saturation of the surface photo-activation was reached. After photo-activation, back-reaction CAMs have been done, with a time step of 6 hours, the samples being kept in darkness between measurements.

X-ray Photoelectron Spectroscopy (XPS) measurements were used to derive surface elemental composition and chemical state of the atomic species in the as-deposited samples. The measurements have been done in a Physical Electronics PHI-VersaProbe 5000 XPS spectrometer (0.5 eV resolution) using the monochromated Al K_α radiation ($h\nu = 1486.6$ eV) and a take-off angle of the photoelectrons of 45°. Prior to XPS measurements, the surface contaminant layer was removed using an Ar^+ ion beam of 40 μA, 1.0 keV. All the XPS peak positions in the survey spectra were calibrated with respect to the C 1*s* peak at the binding energy value of 284.6 eV.

To assess the surface modifications induced by the ex-situ UV irradiation, additional XPS measurements of the sample surface were conducted immediately after super-hydrophilic surface conversion.

Optical transmittance of the films was measured using a double-beam UV-VIS spectrophotometer (Lambda 3, Perkin Elmer). At wavelengths (λ) close to the optical band gap, the fundamental absorption of light dominates over scattering;

therefore we have determined the absorption coefficient, α, from the transmittance spectra according to the equation (Moss, 1959):

$$\alpha(\lambda) = d^{-1} ln(1/T(\lambda)), \tag{3}$$

where d is the film thickness and T – the optical transmittance. The energy dependence of the absorption coefficient, α, is given by the equation (Assim, 2008):

$$(\alpha h\nu)^{1/2} = A_i(h\nu - E_g), \tag{4}$$

where $h\nu$ is the energy of the incident photon, A_i is a parameter independent of the photon energy for the respective transitions, and E_g is the optical band gap.

Results and Discussion

The XRD patterns of the investigated samples (Figure 1) indicate a mixture of anatase and rutile phases. Three of the samples (S.AR1, S.AR2, and S.AR3) have the same anatase weight percentage (46%). The S.RA sample contains 72% rutile, while S.A contains approximately 97% anatase. In sample S.A, additional detectable A(004), A(200), A(105) signals occur, along with the main anatase A(101) feature.

In previous studies, performed on similar samples (Mardare et al., 2008; Dumitriu et al., 2000), it was reported that the titania films prepared under similar conditions, using water vapor, feature higher surface roughness than their oxygen counterparts. On the other hand, we have observed that replacing oxygen with water vapors result in different O and O_2 active species concentration in the discharge plasma, as demonstrated also by Dumitriu et al. (2000). The crystallinity is also directly related to film thickness, due to enhanced conditions for the development of columnar grains, perpendicular to film surface (Chopra, 1969). Consequently, large-size crystallites should be expected to occur in the thicker films S.AR1 and

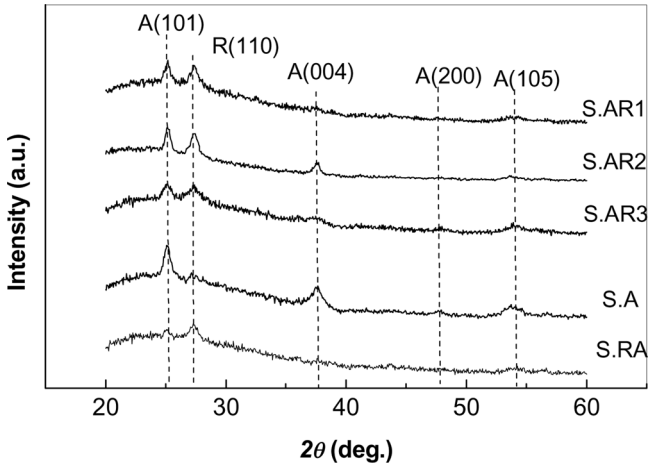

Figure 1. The XRD patterns of the investigated samples.

S.AR2 than in the thinner S.RA sample, all of them deposited at the same substrate temperature.

Despite the fact that the thickness of our samples prepared under water vapor atmosphere is larger than the samples prepared in oxygen, they feature smaller crystallite size (Table I), a result hardly ever discussed in the literature (Jeong et al., 2004). When comparing the structure of the sample S.RA with the thicker samples S.AR3 and S.A we come to a different conclusion. Here, the development of larger crystallites is hindered by the effect of the decreased deposition temperature, which overcompensates for the effect of increasing film thickness.

As shown in Figure 2, relatively smooth film surfaces can be observed in the AFM images, with average rougness values, R_{rms}, below 12 nm (see Table I). This finding agrees with the generally recognized idea that reactive sputtering allows for the growth of uniform smooth films (Ogawa et al., 2008). When comparing the samples S.AR1 and S.AR2, prepared under the same substrate temperature and deposition rate (but of different thickness), one can easily see that the surface roughness is directly proportional to thickness (Table I), in accordance with literature (Chopra, 1969. While the samples S.AR3, S.AR1 and S.AR2 feature the same anatase content, the S.AR3 surface roughness is diminished by a factor of three compared to S.AR1. The difference is again related to the different substrate temperatures during deposition. At lower substrate temperature, smoother films with smaller crystallites size (Table I) can therefore be prepared.

According to our previous studies, the films deposited using oxygen as reactive gas are very smooth (Mardare et al., 2007a; Luca et al., 2007; Mardare et al., 2007b; Mardare et al., 2008; Mardare et al., 2009; Mardare and Hones, 1999), the average surface roughness ranging between 2 and 6 nm (Mardare et al., 2008; Mardare et al., 2009; Mardare and Hones, 1999). The water vapor-deposited samples prepared

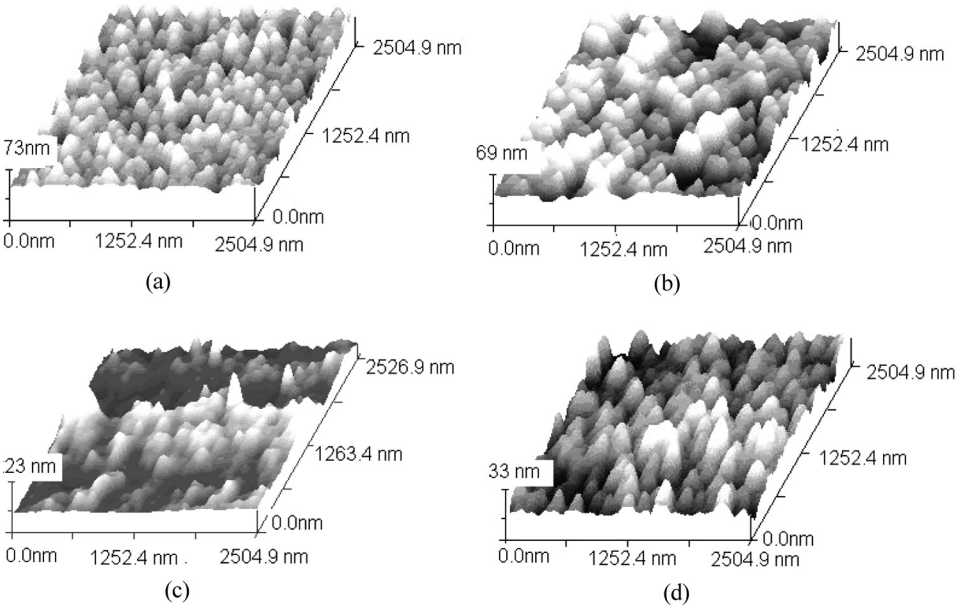

Figure 2. 3-D AFM images of the samples: S.AR1 (a), S.AR2 (b), S.AR3 (c), and S.A (d).

under the experimental conditions presented in the previous section feature higher average roughness values between 8 and 19 nm. The results presented in Table I confirm this observation, despite the fact that oxygen-deposited samples are thinner (Mardare et al., 2008). It is worth mentioning that the secondary ion mass spectrometry results (Dumitriu et al., 2000) indicate the lack of hydrogen atoms in the films deposited under water vapors atmosphere.

The XPS survey spectra of the S.AR1 and S.AR2 samples are shown in Figure 3a. The high-resolution XPS measurements showed that the water vapor as-prepared samples are significantly oxygen-deficient. As a general conclusion, the O/Ti atomic ratios in all samples varies between 1.3 (in S.AR1) and 1.7 (in S.A). The oxygen depletion in the sample surfaces is probably related to elemental composition alteration in the surface induced by high-energy Ar^+ sputtering for contaminant layer removal, prior to XPS measurements (Hashimoto et al., 2004).

Two components, namely a "bulk" component (BE = 530.1 eV in sample S.AR1 and 529.9 eV in sample S.RA, ascribed to the Ti-O bond) and a "surface" component (BE = 531.4 eV and 530,9 eV for the same above-mentioned samples – see Fig. 3(b) and (c), ascribed to a contaminant-like layer (Mardare et al., 2007a)) are present in the narrow scan high-resolution O 1s XPS spectra of the as-prepared samples. The surface component is related to the hydroxyl groups chemisorbed on the surface, withstanding the UHV conditions in the XPS instrument. The concentration ratio of this component (as calculated from the ratio of the area of the surface component and the total area of the O 1s XPS peak) is the largest in the S.AR1 sample (0.39) and the smallest (0.26) in sample S.RA. This can be ascribed to the differences in the photocatalytic activities and hydrophilicity of the samples containing different amounts of anatase phase, as discussed earlier.

To check the origin of the surface component, additional XPS high-resolution spectra of the O 1s core level have been acquired, after the sample surfaces were fully converted to the super-hydrophilic state by UV irradiation. The results are shown in Fig. 3(d) (for the sample S.AR1) and Fig. 3(e) (sample S.RA). Apart from slight modification in binding energy values, significant increase occurs in the concentration values of the surface component, namely 0.43 in sample S.AR1 and 0.36 in sample S.RA (i.e. an increase of 10% and 38% for the two samples, respectively). Note that the after-irradiation atomic concentration of oxygen in the surface layer of the lower anatase content sample remains below the non-irradiated level of the sample S.AR1.

The high-resolution XPS Ti 2p core level peaks of all the as-prepared samples have been deconvoluted into three components: a main Ti^{4+} one, along with Ti^{3+} and small amounts of Ti^{2+} components. Small differences occur among the spectra of the investigated samples (only a single Ti 2p XPS spectrum is shown in Fig. 3(f), as an illustrative example).

To calculate the optical band gap values, E_g, we have extrapolated the linear part of the $(\alpha h\nu)^{1/2} = f(h\nu)$ dependences (derived in all cases from the transmittance spectra) for $\alpha = 0$. Figure 4 shows the curves for some of the investigated samples. A small blue-shift in the band gap adsorption edge can be observed due, probably, to the quantum size effects (see Table I) if one accounts for the known band gap values of anatase and rutile (Hashimoto et al., 2005). The E_g values agree well with the XRD results for the studied samples. It can be easily noticed that the sample containing a significant quantity of rutile phase (S.RA) has the lowest optical energy gap compared to the rest of the samples.

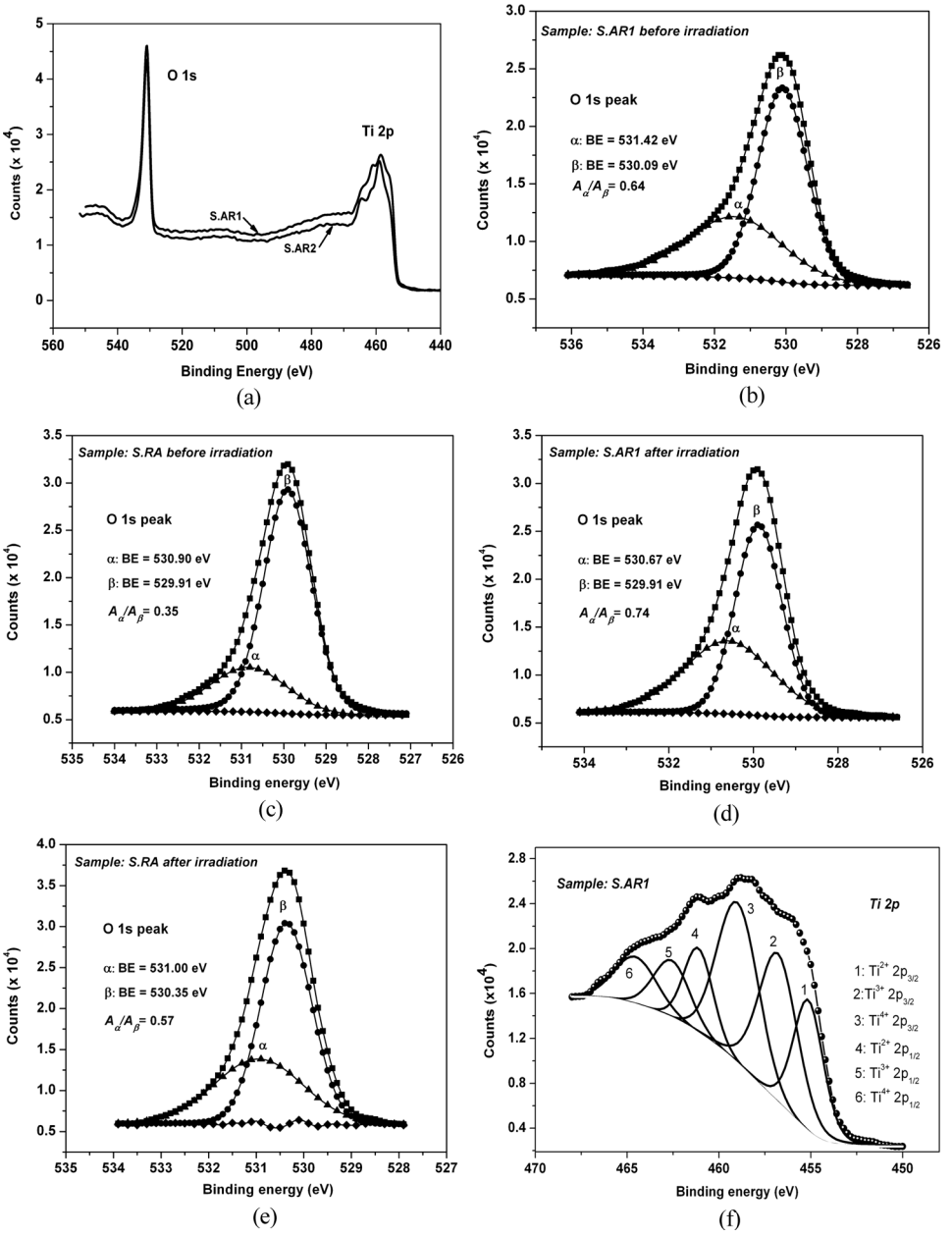

Figure 3. XPS spectra of the investigated samples: (a) the survey spectrum of the samples S.AR1 and S.AR2; (b) the O 1s XPS peak of the as-deposited S.AR1 sample; (c) the O 1s XPS peak of the as-deposited S.RA sample; (d) the O 1s XPS peak of the S.AR1 sample after UV irradiation; (e) the O 1s XPS peak of the S.RA sample after UV irradiation; (f) the Ti 2p XPS peak of the S.AR1 sample.

Figure 5 shows the results of the CAM under UV-irradiation conditions. A sharp decrease in contact angle values occurs for the anatase-rich sample, S.A, namely a drop from 65° to 8° after an UV dose of about 36 J/cm^2. According to

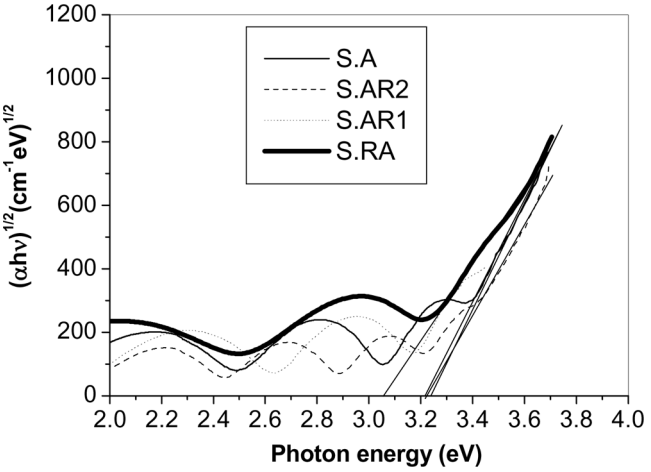

Figure 4. Plots $(\alpha h\nu)^{1/2}$ vs. incident photon energy, $h\nu$. E_g is obtained by extrapolating the linear part of $(\alpha h\nu)^{1/2} = f(h\nu)$ dependence to $(\alpha h\nu)^{1/2} = 0$ (the correlation coefficient of the linear fits is higher than 0.999).

the Wenzel model (1949), the increased surface roughness increases surface wettability of hydrophilic films on behalf of surface tension effects. This is sustained by the initial values of the contact angle of the other samples, which correlate well with the average roughness. For example, the higher-roughness sample S.AR2 compared to the sample S.AR1 features a lower value of the initial contact angle (Fig. 5). It is interesting to compare the hydrophilicity of the samples S.AR1 and S.AR2 with the same anatase content but different roughnesses. The CA values of the films S.AR1 and S.AR2, with an anatase/rutile mixture, reach saturation values higher than 10 deg. (Fig. 5), the rougher one (the thickest) showing better hydrophilic features.

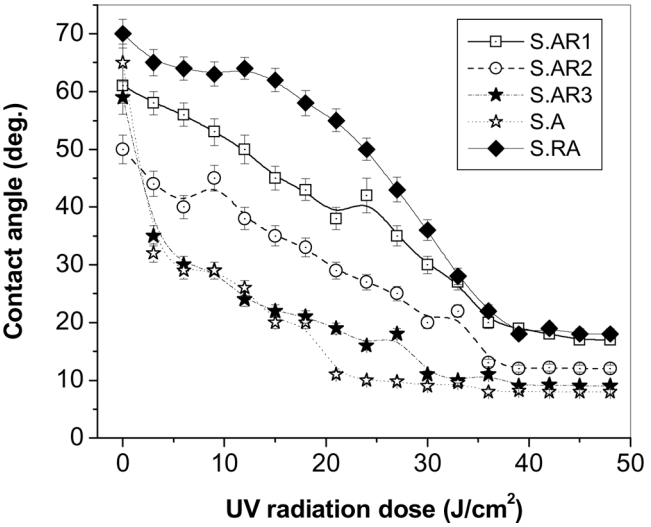

Figure 5. Contact angle vs. UV irradiation dose plots.

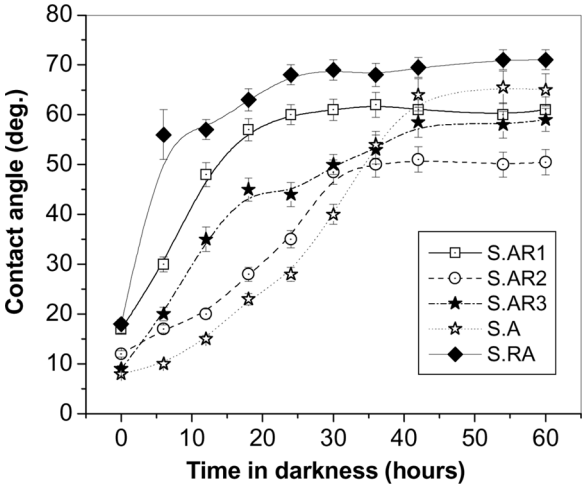

Figure 6. Contact angle vs. time plots under back-reaction regime.

The rougher films performance is directly related to the exposed surface/volume ratio. Although the sample S.AR3 has the same anatase/rutile content as the S.AR1 and S.AR2 and the lowest roughness, its initial CA value is not the highest, but it is closer to that of the sample S.AR1. The sample S.AR3 shows super-hydrophilic properties (CA values of 9° corresponding to an UV dose in excess of 40 J/cm^2). This is due to smaller values of the crystallite size in the sample S.AR3, which in turn leads to higher photocatalytic and hydrophilic activity of the surface (Wenzel, 1949; Bico et al., 1999).

The anatase-rich sample, S.A, also features nano-size crystallites and super-hydrophilic properties. From our set of samples, the oxygen-deposited sample, S.RA, has the worst performance, reaching a CA value of only 18 deg. Comparing with the undoped oxygen-deposited films from our previous studies (Mardare et al., 2007a; Luca et al., 2007; Mardare et al., 2007b), one can see that all these samples can hardly reach CA values of about 10 deg. Here, the explanation is related to three facts: S.RA is very smooth, it has the largest average crystallite sizes, and the highest content of rutile (72%). The lowest energy band gap conditions results in an increased electron-hole recombination rates.

Figure 6 shows the contact angle recovery vs. time during the so-called back-reaction regime, when keeping the samples in darkness after an initial saturation photo-activation. The decay of the photo-activation occurs after time intervals in excess of 40 hours for the super-hydrophilic samples S.A and S.AR3, as a consequence of samples structure and surface conditions. Sample S.RA recovers its initial CA value (about 70 deg.) faster than any other samples under study, confirming its bad photocatalytic performance.

Conclusions

Titanium oxide films containing pure anatase TiO_2 or anatase-rutile phase mixture have been prepared on glass substrates by DC reactive magnetron sputtering, using water vapor as the reactive gas. The effect of both materials' structure and surface

roughness has been investigated and the results were checked against the samples prepared under standard conditions (using oxygen as the reactive gas).

The nano-size crystalline anatase TiO_2 films prepared at the same temperature exhibited increased hydrophilic properties, compared to the films containing the anatase-rutile mixture. On the other hand, by decreasing the substrate temperature from 573 K to 463 K the hydrophilic performance of the anatase-rutile mixture films becomes comparable to that of pure anatase. This is related to the development of smaller size crystallites favored by the conditions of lower substrate temperature.

The intrinsic titania hydrophilicity is enhanced by surface roughness, due to the effect of a more open surface topography, and film thickness. In contrast with the sputtered titania films classically grown (using oxygen as reactive gas), finer grained films featuring rougher surface have been prepared using water vapors as reactive gas. These samples are superior in achieving the best hydrophilic properties.

Acknowledgements

The financial support from the CNCSIS Contract PCCE-ID_76 is acknowledged by D. Mardare, A. Manole and D. Luca. A. Yildiz acknowledges the 2218-coded Turkish national research scholarship. D. Mardare is grateful to Prof. F. Lévy from the Polytechnic Federal School of Lausanne, Switzerland, for ensuring the access to deposition facilities.

References

Assim, E. M. (2008). Optical constants of titanium monoxide TiO thin films, *J. Alloys and Compounds*, **465**(1–2), 1–7.

Bico, J., Marzolin, C., Qu, D. (1999). Pearl drops, *Europhys. Lett.*, **47**, 220–226.

Chopra, K.L. (1969) *Thin Film Phenomena*, McGraw-Hill, New York, p. 185.

Dumitriu, D., Bally, A. R., Ballif, C., Hones, P., Schmid, P. E., Sanjines, R., and Levy, F. (2000). Photocatalytic degradation of phenol by TiO_2 thin films prepared by sputtering, *Appl. Catal. B: Environ.*, **25**, 83–92.

Fujishima, A., Hashimoto, K., and Watanabe, T. (1999). *TiO_2 Photocatalysis. Fundamentals and Applications*, BKC Inc., Tokyo.

Hao, W.C., Zheng, S.K., Wang, C., and Wang, T.M. (2002).Comparison of the photocatalytic activity of TiO_2 powder with different particle size, *J. Mater. Sci. Lett.*, **21**(20), 1627–1629.

Hashimoto, K., Irie, H., and Fujishima, A. (2005). TiO_2 Photocatalysis: A historical overview and future prospects, *Jpn. J. Appl. Phys.*, **44**(12), 8269–8285.

Hashimoto, S., Tanaka, A., Murata, A., and Sakurada, T. (2004). Formulation for XPS spectral change of oxides by ion bombardment as a function of sputtering time, *Surf. Sci.*, **556**(1), 22–32.

Klug, P., and Alexander, L. E. (1974). *X-ray Diffraction Procedures*, Wiley, New York: p. 515.

Jeong, B. S., Norton, D. P., Budai, J. D., and Jellison, G. E. (2004). Epitaxial growth of anatase by reactive sputter deposition using water vapor as the oxidant, *Thin Solid Films*, **446**, 18–22.

Luca, D., Teodorescu, C. M., Apetrei, R., and Mardare, D. (2007). Preparation and characterization of increased efficiency photocatalytic $TiO_{2-x}N_x$ thin films, *Thin Solid Films*, **515**, 8605–8610.

Mardare, D., Luca, D., Teodorescu, C. M., and Macovei, D. (2007a). On the hydrophilicity of nitrogen-doped TiO_2 thin films, *Surface Science*, **601**, 4515–4520.

Mardare, D., Iacomi, F., and Luca, D. (2007b). Substrate and Fe-doping effects on the hydrophilic properties of TiO_2 thin films, *Thin Solid Films*, **515**, 6474–6478.

Mardare, D., Tasca, M., Delibas, M., and Rusu, G. I. (2000). On the structural properties and optical transmittance of TiO_2 R.F. sputtered thin films, *Appl. Surf. Sci.*, **156**, 200–206.

Mardare, D., Iftimie, N., and Luca, D. (2008). TiO_2 thin films as sensing gas materials, *Journal of Non-Crystalline Solids*, **354**, 4396–4400.

Mardare, D., Cornei, N., and Rusu, G. I. (2009). On the properties of nanostructured titanium oxide thin films, *Superlattices and Microstructures*, **46**, 209–216.

Mardare, D., and Hones, P. (1999). Optical dispersion analysis of TiO_2 thin films based on variable-angle spectroscopic ellipsometry measurements, *Mat. Sci. Eng. B*, **68**(1), 42–47.

Moss, T. S. (1959). *Optical Properties of Semiconductors*, Butterworth, London, p.175.

Musil, J., Heřman, D., and Šícha, J. (2006). Low-temperature sputtering of crystalline TiO_2 films, *J. Vac. Sci. Technol.*, **24**(3), 521–528.

Ogawa, H., Higuchi, T., Nakamura, A., Tokita, S., Miyazaki, D., Hattori, T., and Tsukamoto, T. (2008). Growth of TiO_2 thin film by reactive RF magnetron sputtering using oxygen radical, *J. Alloys Compounds*, **449**(1–2), 375–378.

Ollis, D. F., Al-Ekabi, H., eds. (1993). *Photocatalytic Purification and Treatment of Water and Air*, Elsevier, Amsterdam.

Ruzycki, N., Herman, G. S., Boatner, L. A., and Diebold, U. (2003). Scanning tunneling microscopy study of the TiO_2 anatase (100), *Surf. Sci. Lett.*, **529**(1–2), L239–244.

Shirolkar, M., Abyaneh, M. K., Singh, A., Tomer, A., Choudhary, R., Sathe, V., Phase, D., and Kulkarni, S. (2008). Rapid switched wettability of titania films deposited by dc magnetron sputtering, *J. Phys. D: Apple. Phys.*, **41**, 155308–155316.

Spurr, R. A., and Myers, H. (1957). Quantitative analysis of anatase-rutile mixtures with an X-ray diffractometer, *Anal. Chem.*, **29**, 760–762.

Wenzel, R. N. (1949). Surface roughness and contact angle, *J. Phys. Colloid. Chem.*, **53**, 1466–1467.